



HAL
open science

Speckle reduction with multitaper approach to improve B/A imaging

Matthieu Toulemonde, François Varray, Piero Tortoli, Christian Cachard,
Olivier Basset

► **To cite this version:**

Matthieu Toulemonde, François Varray, Piero Tortoli, Christian Cachard, Olivier Basset. Speckle reduction with multitaper approach to improve B/A imaging. Acoustics 2012, Apr 2012, Nantes, France. hal-00810810

HAL Id: hal-00810810

<https://hal.science/hal-00810810>

Submitted on 23 Apr 2012

HAL is a multi-disciplinary open access archive for the deposit and dissemination of scientific research documents, whether they are published or not. The documents may come from teaching and research institutions in France or abroad, or from public or private research centers.

L'archive ouverte pluridisciplinaire **HAL**, est destinée au dépôt et à la diffusion de documents scientifiques de niveau recherche, publiés ou non, émanant des établissements d'enseignement et de recherche français ou étrangers, des laboratoires publics ou privés.



ACOUSTICS 2012

Speckle reduction with multitaper approach to improve B/A imaging

M. Toulemonde^{a,b}, F. Varray^a, P. Tortoli^c, C. Cachard^a and O. Basset^a

^aCentre de recherche en applications et traitement de l'image pour la santé, 7 avenue Jean Capelle, Bat Blaise Pascal, 69621 Villeurbanne Cedex

^bDepartment of Electronics and Telecommunications [Florence], Via S. Marta, 3 50139 Firenze

^cUniversità degli studi di Firenze, Via S. Marta, 3, 50139 Firenze, Italy
matthieu.toulemonde@creatis.univ-lyon1.fr

During the propagation of an ultrasound wave, harmonic frequencies appear due to the nonlinear property of the tissue. When tissue characterization is concerned, the non-linear parameter B/A can be interesting to differentiate normal and pathological tissues. Determination of the B/A parameter using a new extended comparative method (ECM) is limited by the presence of the speckle noise. Using multitaper approach, we show that it is possible to improve the B/A determination from simulated data provided by the software CREANUIS.

1 Introduction

Nowadays, clinical ultrasound imaging is a common diagnostic tool thanks to its non-invasive behavior and a relatively cheap equipment. In this study, two new techniques are developed to improve the quality of ultrasound images and to allow tissue characterization.

The first technique attempts to improve the image quality. Ultrasound B-mode images exhibit a granular texture called speckle. To reduce this phenomenon, different techniques can be used such as frequency [1] or spatial compounding [2]. The drawback of these techniques comes from the different acquisitions that are required at different frequencies, respectively position, to average images with different speckle and the reduced frame rate induced. A novel approach [3] based on Thomson's multitaper permits to save the frame rate and to improve ultrasound image quality.

The second technique proposed is based on the nonlinear property of ultrasound. During the propagation of an ultrasound wave, harmonic frequencies appear due to the nonlinear property of the tissue. The nonlinear parameter B/A of the medium is one of the important parameter which influence harmonics amplitude creation. When tissue characterization is concerned, the B/A parameter show different values between normal and pathological tissues [4]-[6]. Several methods are used to measure the B/A parameter and can be regrouped in two main families: thermodynamic and finite amplitude approaches [7]. Thermodynamic methods have a good accuracy but needs specific material instead of the finite amplitude approaches which can be used in echo mode situation. A recent paper [8] proposes an extended comparative method (ECM) to image the B/A parameter in inhomogeneous nonlinear media. However, the accuracy of this approach is limited by the presence of speckle in the image.

In this paper, we propose to improve the measurement of B/A parameter using ECM after the implementation of the Thomson's multitaper approach. Indeed, thanks to the improvement of the obtained fundamental and second-harmonic images, the B/A estimation is facilitated and the improvement of such image beamforming is directly evaluated.

This paper is organized as follows. In the next section, multitaper method is presented and also comparative experiments to show effectiveness of the approach to denoise B-mode image. Then, the ECM technique to calculate B/A parameter is introduced. The evaluation of multitaper method is achieved to estimate B/A parameter. Finally, a discussion and a conclusion close the paper.

2 Multitaper method

2.1 Theory

The multitaper method is based on Thomson's multitaper approach [9] which is used for power spectrum

estimations. In [3], the authors applied this approach to the spatial domain.

In echographic image, a probe, which is a multi-element transducer, is used for both transmitted and received mode. In order to obtain the global pressure wave backscattered by the medium, the probe is subdivided on sub-part. Appropriate delays and window apodization are supplied on a sub-part to focus a wave field in both cases. At reception, the received signal is summed to create the radio frequency (RF) line. The RF image is obtained by repeating the same operation on each sub-part.

When a single taper (e.g. Hanning window) is used in reception mode, a part of the spatial spectrum is discarded. In the multitaper approach, different orthogonal tapers are used. The information discarded by one taper is partially recovered by another taper and each taper extracts a different part of the spatial spectrum. For the frequency response, it corresponds to synthesize a wider main lobe which maximizes the power in the main lobe and reduces side lobe leakage. RF images obtained with these tapers permit to obtain different speckle realization. By averaging the set of B-mode images obtained by envelope detection of each RF images, the speckle is then reduced.

The tapers must be orthogonal to minimize variance and optimally concentrated in frequency to minimize bias [9]. It means that tapers extract energy around the spatial frequency of interest, in a frequency interval corresponding to the main lobe.

Discrete prolate spheroidal sequences (DPSS) or Slepian sequences are optimal tapers satisfying these requirements. DPSS tapers are obtained by taking the eigenvectors of the Toeplitz matrix [9]:

$$D_{n,m} = \frac{\sin 2\pi BW(n-m)}{\pi(n-m)}, \quad n, m = 0, 1, \dots, N-1 \quad (1)$$

where BW corresponds to the frequency band and N the number of samples (size of tapers). DPSS tapers are ordered by their eigenvalues. If their eigenvalues are close to one, spectra of DPSS tapers in the frequency interval is high otherwise, if they are close to zero, spectra of DPSS tapers in the frequency interval is low.

Figure 1 shows three selective DPSS tapers for $N=64$ and $N \times BW = NBW = 4$, with their eigenvalues equal to one, in order to have a synthesize filter with a frequency response presented in Figure 2. This synthesize DPSS filter is compared to a Hanning apodization. Hanning taper is used as reference apodization because it is the classical apodization used in echography image. Figure 2 shows that the main lobe of the DPSS apodization is wider than the Hanning apodization.

Considering that the size of tapers is fixed, the number of tapers depends on the NBW parameter. Higher is the NBW parameter, higher is the number of tapers and so wider is the main lobe.

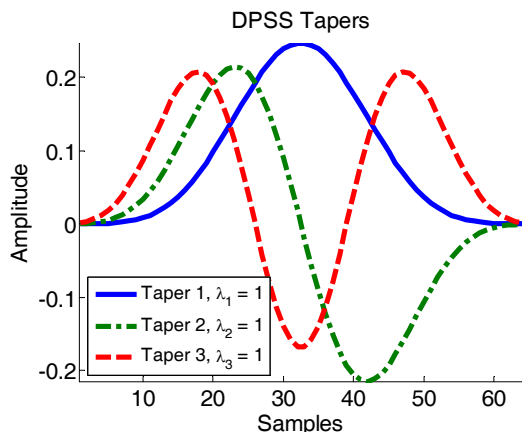


Figure 1: Selective DPSS tapers for $N = 64$ and $NBW = 4$ with their λ_k eigenvalues.

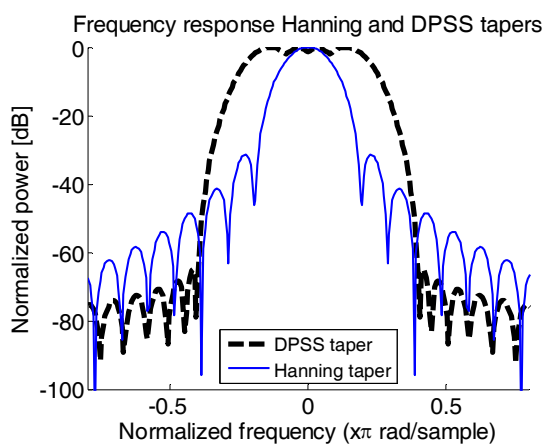


Figure 2: Frequency response of Hanning and synthesize DPSS, with three tapers.

2.2 Speckle reduction experiments

In order to test the new multitaper approach, we use the software CREANUIS [10] to simulate second-harmonic nonlinear RF images. The objective of this simulation is to determine the effectiveness of the multitaper compared to the original signal and a filter bank speckle denoising technique. The simulated medium is a cyst phantom [11] with 100 000 scatterers randomly placed (Figure 3.f). The probe parameters used in all simulations are summarized in Table 1.

Table 1: Probe parameters used in simulation

Parameter	Value
Pitch	245 μm
Kerf	30 μm
Height	6 mm
Elevation focus	23 mm
Number of active elements	64

A 3-cycle sinusoidal burst at 3 MHz with a Hanning window, focused at 70 mm, was transmitted. In transmission and reception, a Hanning apodization has been used.

From the same simulations, three different image processing approaches have been implemented. First, the classical ultrasound image beamforming has been performed. Secondly, the multitaper approach has been

used instead of the Hanning apodization. The average image has been created from three DPSS tapers. The last strategy is based on the application of a filter bank to denoise the image. It consists in slicing the reception signal in different bandwidth of 2 MHz with 5th Butterworth filter in step of 1 MHz. After a compensation of the depth attenuations, depending of the frequency, an envelope detection for each sub-band is conducted and then, resulting images are summed. To evaluate the effectiveness of the multitaper and the decrease of the speckle, the signal-to-noise ratio (SNR) is computed in a region-of-interest (ROI) of 5 mm² (Figure 3.f):

$$SNR = \mu/\sigma \quad (2)$$

where μ is the signal mean and σ the standard deviation

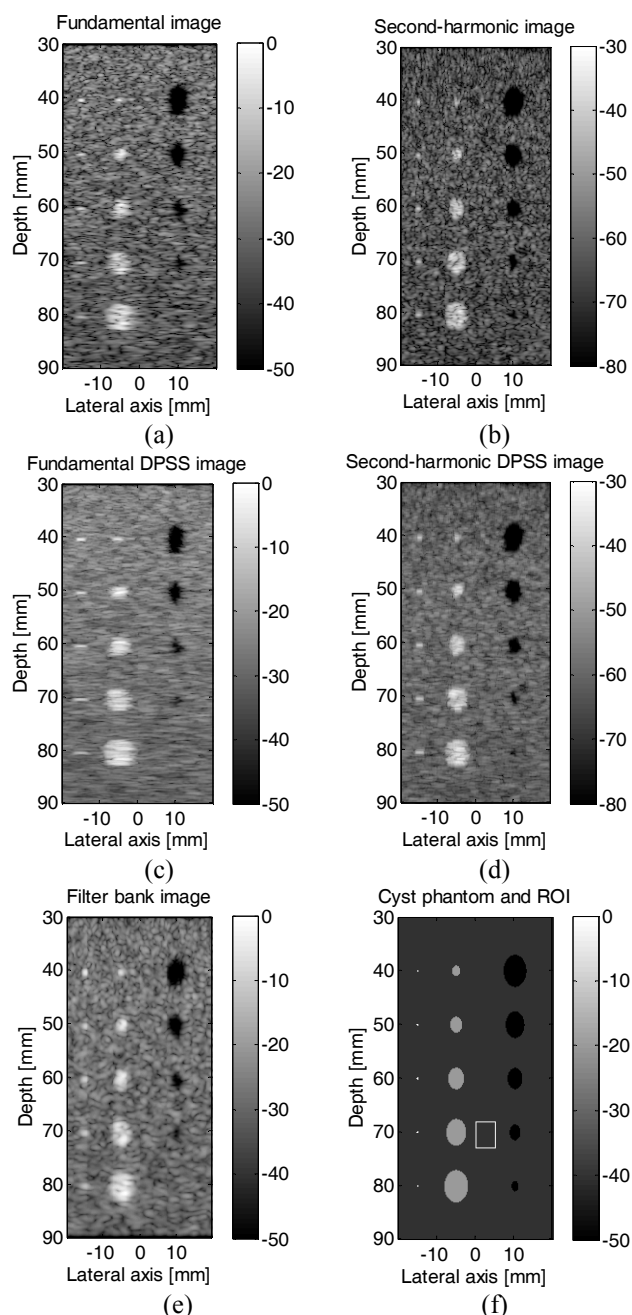


Figure 3: CREANUIS log-compressed (dB) image simulated (a) fundamental image and (b) second harmonic images, (c) fundamental DPSS image and (d) second harmonic DPSS images, (e) filter bank image and (f) cyst phantom scatterer's amplitude and ROI.

Table 2: Signal-to-noise ratio (SNR) and resolution

Approach	SNR	Axial resolution (mm)	Lateral resolution (mm)
Fundamental image	2.60	0.38	1.69
Second harmonic image	2.23	0.47	0.90
Fundamental DPSS image	5.14	0.43	2.36
Second harmonic DPSS	4.04	0.54	1.26
Filter bank image	3.36	0.74	1.65

The obtained simulated images and results are given in Figure 3 and Table 2, respectively. The use of multitaper and filter bank permits to denoise the image. This is clearly visible in fundamental image in Figure 3.c and Figure 3.e. However, lateral and axial resolutions are reduced. The more resolution value it is (Table 2), the less precision it is to differentiate a scatterer. Unlike the filter bank method, the multitaper method permits to display the second harmonic (Figure 3.d) which leads to an increase of the lateral resolution.

Another experiment was realized to compare the SNR as a function of the number of DPSS tapers. Results given in Table 3 show that SNR increases with tapers number and tends to a limit. In term of resolution, lateral and axial resolutions decrease, as the number of tapers increases.

Table 3: Comparison of SNR for different DPSS tapers number

Number of tapers	NBW	SNR fundamental	SNR second harmonic
3	1.5	5.14	4.04
5	2.5	6.67	6.00
7	3.5	7.15	7.51
10	5	7.31	7.90
13	6.5	7.37	8.16
15	7.5	7.40	8.35

3 Extended Comparative Method

The B/A parameter could be related to the Taylor series expansion of the pressure wave $p = p(\rho, s)$ in a medium with constant entropy $s = s_0$ [12]:

$$p - p_0 = \left(\frac{\partial p}{\partial \rho} \right)_{0,s} (\rho - \rho_0) + \left(\frac{\partial^2 p}{\partial \rho^2} \right)_{0,s} \frac{(\rho - \rho_0)^2}{2} + \dots \quad (3)$$

where ρ is the density of the medium, p_0 and ρ_0 are the pressure and density values at equilibrium. Equation (3) is simplified using $P = p - p_0$ and $\rho' = \rho - \rho_0$:

$$P = A \frac{\rho'}{\rho_0} + \frac{B}{2!} \left(\frac{\rho'}{\rho_0} \right)^2 + \dots \quad (4)$$

$$A = \rho_0 \left(\frac{\partial P}{\partial \rho} \right) \equiv \rho_0 c_0^2 \quad (5)$$

$$B = \rho_0^2 \left(\frac{\partial^2 P}{\partial \rho^2} \right) \quad (6)$$

The B/A ratio can be expressed as a function of the sound velocity c_0 and the density of the medium from (5) and (6):

$$\frac{B}{A} = \frac{\rho_0}{c_0^2} \left(\frac{\partial^2 P}{\partial \rho^2} \right) \quad (7)$$

In the literature, the nonlinear coefficient β , which is related to B/A , is also used, $\beta = 1 + B/2A$.

The extended comparative method (ECM) [8] finds its origin in insertion-substitution method developed in [13]. The objective is to compare a reference medium with a known nonlinear coefficient β_0 and another medium with an unknown nonlinear coefficient β_i . ECM is based on the expression of the amplitude pressure of the second-harmonic wave p_2 which is expressed as [13]:

$$p_2(z) = \frac{\pi f p_0^2}{\rho_0 c_0^3} \int_0^z \beta(u) \exp \left(\int_0^u -2\alpha_1(v) dv - \int_u^z \alpha_2(v) dv \right) du \quad (8)$$

where α_1 and α_2 are attenuation coefficients of respectively fundamental and second-harmonic wave of the medium.

In the case of a homogeneous nonlinear coefficient and attenuation in the reference medium, equation (8) could be expressed as [8]:

$$p_{20}(z) = \frac{\beta_0 \pi f p_0^2}{\rho_0 c_0^3} I_0(z) \quad (9)$$

where

$$I_0(z) = \frac{e^{-2\alpha_{10}z} - e^{-\alpha_{20}z}}{\alpha_{20} - 2\alpha_{10}} \quad (10)$$

Based on the comparative method, the ratio between the amplitude pressure of the second harmonics of the unknown medium, subscript i , and the reference medium, subscript 0, gives:

$$\frac{p_{2i}(z)}{p_{20}(z)} = \frac{\rho_0 c_0^3}{\rho_i c_i^3} \frac{e^{\int_0^z -\alpha_{2i}(v) dv} \int_0^z \beta_i(\mu) e^{\left(\int_0^{\mu} (\alpha_{2i}(v) - 2\alpha_{1i}(v)) dv \right)} d\mu}{\beta_0 I_0(z)} \quad (11)$$

$$\frac{\beta_i(z)}{\beta_0} = \frac{\rho_i c_i^3}{\rho_0 c_0^3} \left[V(z) \frac{dp_{2i}/p_{20}}{dz} + W(z) \frac{p_{2i}}{p_{20}} \right] \quad (12)$$

where V and W are two terms depending on attenuations of the two different media:

$$V(z) = I_0(z) e^{\int_0^z 2\alpha_i(v) dv}$$

$$W(z) = \frac{e^{-\alpha_{10}z} (\alpha_{2i}(z) - 2\alpha_{10}) - e^{-\alpha_{20}z} (\alpha_i(z) - \alpha_{20})}{\alpha_{20} - 2\alpha_{10}} e^{\int_0^z 2\alpha_i(v) dv} \quad (13)$$

4 Evaluation of DPSS taper on B/A estimation

As shown in the previous section, the measurement of the nonlinear coefficient β_i , and so the nonlinear parameter B/A , requires the second harmonic pressure. However, during a clinical exam, only RF images or B-mode images are acquired.

The hypothesis of the technique considers that the intensity of B-mode images is related to the local pressure field if the effects of scatterers are successfully suppressed.

It is mean that the detectability of the local texture changes in the B-mode image corresponding to the local pressure and can be improve by reducing the speckle noise.

Two different techniques are tested to extract from the RF image information corresponding to the second harmonic pressure: alternating sequential filter (ASF) and multitaper method. Both methods permit to decrease the speckle noise. ASF is based on mathematical morphology [14] operations. It consists in the composition of increasingly severe openings and closings.

As previously explain, the multitaper method is applied on the RF signal as tapers to do beamforming. Then, 5th Butterworth filters and envelop detection are used to obtain fundamental and second harmonic filtered B-mode images. ASF technique is used on pre-filtered fundamental and second harmonic B-mode images. In second-harmonic image, scatterer's amplitude variations depend on the nonlinear parameter and also from scatterer's distribution. This is not the case in the fundamental image where scatterer's amplitude depends only from the scatterer's distribution. For both cases, the normalization of the second harmonic image by the fundamental image permits to suppress variation coming from the scatterer's distribution. In order to obtain the final second-harmonic pressure, a low pass filter is used to reduce the high frequency information. It is then used to do the ratio image with the reference medium which is a part of the same image.

CREANUIS software has been used to test the multitaper method. The same probe characteristics are used (Table 1) and a 3-cycle sinusoidal signal burst at 3 MHz with a Hanning window, focused at 70 mm, was transmitted in the medium. In transmission, Hanning apodization has been used but none on reception. Two different medium are simulated. The first is a medium with a homogeneous distribution of 622 000 scatterers. There are randomly defined in space and amplitude. The second is a medium with inhomogeneous distribution of scatterers. 460 000 scatterers are on the negative x axis and 310 000 on the positive. Both media have the same nonlinear parameter map, as described in Figure 4. These two different scatterer's media are chosen in order to prove that ECM is effective to estimate the nonlinear parameter on arbitrary medium. In the Figure 4, the region between the two vertical lines is considered as the reference medium used in equation (12). Either seven DPSS tapers or ASF are used to decrease the speckle noise. This choice is related to the results in Table 3 where seven DPSS tapers permit to have a good SNR.

The resulting B-mode second-harmonic images for the two techniques in the homogeneous medium are displayed in Figure 5.a and Figure 5.b and in the inhomogeneous medium in Figure 6.a. and Figure 6.b. In the left part of the Figure 6.a, the signal backscattered by the tissue is higher due to the increase of the scatterer's density.

For the nonlinear homogeneous medium, the resulting images and statistical estimation of B/A measured on different regions with different technics are given in Figure 5.c, Figure 5.d and Table 4. For the nonlinear inhomogeneous medium, results are given in Figure 6.c, Figure 6.d and Table 5.

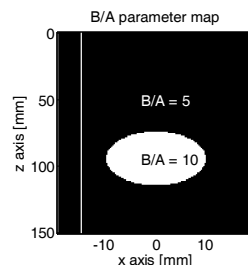


Figure 4: Nonlinear parameter map. The region between the two vertical lines is considered as the reference medium.

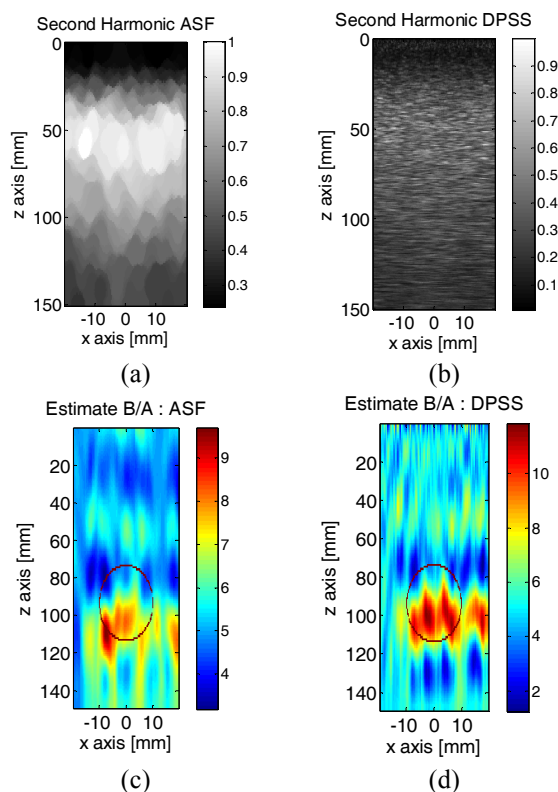
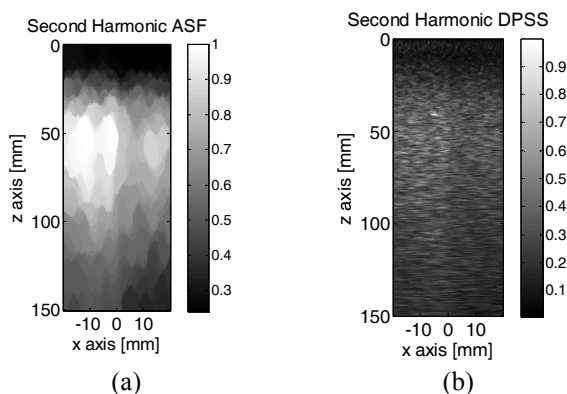


Figure 5: Homogeneous medium, second harmonic filtered image for (a) ASF and (b) DPSS, the resulting B/A image for (c) ASF and (d) DPSS.

Table 4: Evaluation of B/A estimated in homogeneous scattering medium

Method	Set B/A	Mean value of B/A	Standard deviation of B/A
ASF	5	5.45	0.91
	10	6.55	1.28
DPSS	5	5.15	1.47
	10	8.15	2.45



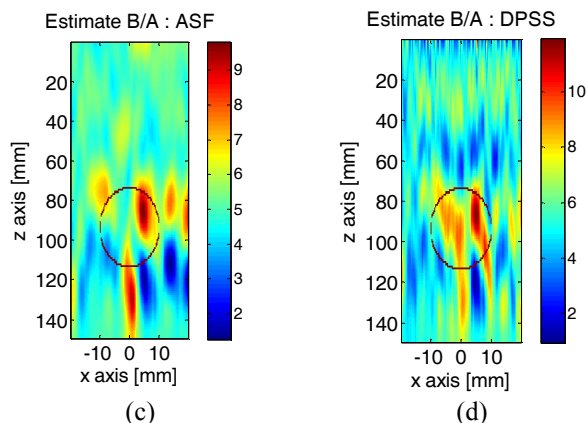


Figure 6: Inhomogeneous medium, second harmonic filtered image for (a) ASF and (b) DPSS, the resulting B/A image for (c) ASF and (d) DPSS.

Table 5: Evaluation of B/A estimated in inhomogeneous scattering medium

Method	Set B/A	Mean value of B/A	Standard deviation of B/A
ASF	5	5.05	1.01
	10	5.82	1.45
DPSS	5	5.37	1.22
	10	7.42	1.79

As shown by results, the DPSS approach provides a better estimation of the B/A parameter compared with ASF method. In ASF's B/A figure, it is observable that the method spreads out the region with high B/A parameter because, the ASF method smooths more than the DPSS method. This is noticeable when second harmonic ASF figures are compared with second harmonic DPSS ones for both homogeneous and inhomogeneous medium. This is also why the B/A estimated value is lower for ASF techniques and B/A ASF figures look more homogeneous.

5 Discussions and conclusions

It was demonstrated that Thomson's multitaper approach permits to reduce the speckle noise whereas decreasing lateral and axial resolution. A compromise has to be found between increasing the SNR and decreasing the resolution.

Combined to the new ECM method to estimate B/A parameter in B-mode images, the multitaper approach improves the estimation of the B/A parameter in comparison with ASF method. Even if an inhomogeneous scatterer's media is used and the estimation of B/A parameter decreased, the multitaper approach allows a better localisation of the high B/A area than the ASF technique.

Currently, the B/A estimation with ECM combined with the multitaper method was only made in simulation. The non-existence of phantom with a known and fixed B/A parameter prevents to test correctly the method.

Acknowledgments

Special thanks are due to the Centre Lyonnais d'Acoustique (CeLyA), ANR grant n°2011-LABX-014.

References

- [1] Y. Erez, Y.Y. Schechner, D. Adam, "Ultrasound Image Denoising by Spatially Varying Frequency Compounding", *Proc. DAGM Symposium, Lecture notes on computer science*, vol. 4147, pp. 1-10, 2006.
- [2] S.K. Jespersen, J.E. Wilhjelm, H. Sillesen, "Ultrasound Spatial Compound Scanner for Improved Visualization in Vascular Imaging", in *IEEE Ultrasonics Symposium*, Sendai, 1998.
- [3] A.C. Jensen, C.I.C. Nilsen, A. Austeng, S.P. Næsholm, S. Holm, "A Multitaper Approach to Speckle Reduction for Medical Ultrasound Imaging", in *IEEE Ultrasonics symposium*, San Diego, 2010.
- [4] X. Gong, Z. Zhu, T. Shi, J. Huang, "Determination of the acoustic nonlinearity parameter in biological media using FAIS and ITD methods", *J. Acoust. Soc. Am.*, vol. 86, no. 1, pp. 1-5, 1989.
- [5] W. K. Law, L.A Frizzell, F. Dunn, "Determination of the nonlinearity parameter B/A of biological media", *Ultrasound in Med. & Biol.*, vol. 11, no. 2, pp. 307-318, 1985
- [6] X. Gong, D. Zhang, J. Liu, H. Wang, Y. Yan, X. Xu, "Study of acoustic nonlinearity parameter imaging methods in reflection mode for biological tissues", *J. Acoust. Soc. Am.*, vol. 116, no. 3, pp. 1819-1825, 2004.
- [7] W.K. Law, L.A. Frizzell, F. Dunn, "Comparison of thermodynamic and finite amplitude methods of B/A measurement in biological materials", *J. Acoust. Soc. Am.*, vol. 74, no. 4, pp. 1295-1297, 1983.
- [8] F. Varray, O. Basset, P. Tortoli, C. Cachard, "Extensions of Nonlinear B/A Parameter Imaging Methods for Echo Mode", *IEEE Trans. UFFC*, vol. 58, no. 6, pp. 1232-1244, 2011.
- [9] D. J. Thomson, "Spectrum estimation and harmonic analysis", *Proceedings of the IEEE*, vol. 70, no. 9, pp. 1055-1096, 1982.
- [10] F. Varray, C. Cachard, P. Tortoli, O. Basset, "Nonlinear Radio Frequency Image Simulation for Harmonic Imaging: CREANUIS", in *IEEE Ultrasonics symposium*, San Diego, 2010.
- [11] J.A. Jensen, P. Munk, "Computer phantoms for simulating ultrasound B-Mode and CFM images", *Acoustical Imaging*, vol. 23, pp. 75-80, 1997.
- [12] R.T. Beyeyr, "Parameter of Nonlinearity in Fluids", *J. Acoust. Soc. Am.*, vol 32, no. 6, pp. 719-721, 1960.
- [13] D. Zhang, X. Gong, S. Ye, "Acoustic nonlinearity parameter tomography for biological specimens via measurements of the second harmonics", *J. Acoust. Soc. Am.*, vol. 99, no. 4, pp. 2397-2402, 1996.
- [14] S.R. Sternberg, "Grayscale Morphology", *Computer Vision, Graphics, and Image Processing*, vol. 35, no. 3, pp. 333-355, 1986.